

Quadrupolar second-harmonic generation by helical beams and vectorial vortices with radial or azimuthal polarization

Miguel G. Mandujano and Jesús A. Maytorena*

*Centro de Nanociencias y Nanotecnología, Universidad Nacional Autónoma de México,
Apartado Postal 2681, 22800 Ensenada, Baja California, México*

(Received 5 April 2013; published 7 August 2013)

We study the optical second-harmonic radiation (SHG) generated by scattering from a homogeneous centrosymmetric thin composite material illuminated by higher-order Gaussian laser beams. The induced second-order source polarization is taken as of quadrupolar type $(\mathbf{E} \cdot \nabla)\mathbf{E}$, which depends on the inhomogeneity of the incident electric field \mathbf{E} . This nonlinear source has the same form as that responsible of the SH signal observed in a composite made of Si nanocrystals embedded uniformly in a SiO_2 matrix and that calculated for a thin disordered array of nanospheres. We calculate the SH radiation angular patterns generated by several incident combinations of spatial modes and states of polarizations. In particular, excitation with radially and azimuthally polarized doughnut modes and helical beams carrying orbital angular momentum with linear or circular polarization are considered. We found that this quadrupolar SHG depends sensitively on the transverse structure and polarization of the driving field. The response to $\nabla\mathbf{E}$ introduces a factor $\mathbf{E}(\mathbf{E} \cdot \mathbf{K})$ in the Fourier component of the SH scattering amplitude, absent in electric-dipole-allowed SHG, that can give additional nodal lines or rings in the SH angular patterns, changes of the state of polarization, or additional azimuthal phases in the harmonic radiation. For circularly polarized beams with helical phase wave front, we found a selection rule according to which the nonlinear scattering of an optical vortex with charge l_ω and spin $\sigma = \pm 1$ induces a SH vortex field with a spin-dependent charge doubling $l_{2\omega} = 2l_\omega + \sigma$. These features may be useful to identify SHG processes of quadrupolar nature and suggest a way to produce scattered SH radiation with a desired angular pattern and state of polarization.

DOI: [10.1103/PhysRevA.88.023811](https://doi.org/10.1103/PhysRevA.88.023811)

PACS number(s): 42.65.Ky, 78.66.-w, 03.50.De

I. INTRODUCTION

Second-harmonic generation (SHG) is a well-known nonlinear optical probe of planar surfaces and interfaces of centrosymmetric systems [1–7]. The surface sensitivity stems from the strong suppression of the dipolar second-order bulk polarization due to symmetry. At the surface the inversion symmetry is broken and an electric dipolar SH response $P_i^{(2)} = \chi_{ijk}^s E_j E_k$ then becomes allowed. There is, however, a residual bulk contribution of quadrupolar character originated from the inhomogeneity of the incident electric field $\mathbf{P}_Q^{(2)} \propto (\mathbf{E} \cdot \nabla)\mathbf{E}$.

Besides flat surfaces, SHG scattering has recently been introduced to study the surface of micro- and nanoparticles [8]. For a spherical nanoparticle the centrosymmetry is locally lost at its surface and therefore a nonlinear surface polarization is induced. However, centrosymmetry is globally recovered, leading to a null total dipole moment unless the field were inhomogeneous [9,10]. Thus, to leading order in the field gradient, the nonlinear induced dipole has the nonlocal form $\mathbf{p}^{(2)} = \gamma^e (\mathbf{E} \cdot \nabla)\mathbf{E} + \gamma^m \mathbf{E} \times (\nabla \times \mathbf{E})$ whose radiation may be comparable to that of the nonlinear quadrupole polarization $\mathbf{P}_Q^{(2)} = \gamma^q \nabla \cdot \mathbf{E}\mathbf{E}$, where the γ 's are given functions of the dipole surface susceptibilities and quadrupole bulk susceptibilities of the constitutive material. This is in contrast to the dipolar SHG from planar geometry.

Si nanocrystals (NCs) embedded in glass provide another relevant example where quadrupole contributions (field gradient) also play an important role in the SHG surface

response. The observation of SHG from a thin composite layer made up of Si spherical NCs (~ 5 nm) within a SiO_2 matrix demonstrated the sensitivity of this nonlinear optical process to the Si/ SiO_2 interface, even for a macroscopically centrosymmetric system [11,12]. To explain the measured angular distribution of harmonic radiation, a theory of SHG from a thin homogeneous slab of a composite medium made up of an array of centrosymmetric spheres excited by an arbitrary nonhomogeneous electromagnetic field was developed [10]. It was found that the leading radiating part of the macroscopic quadratic polarization of the nanocomposite can be written as $\mathbf{P}^{(2)} = \Delta' (\mathbf{E} \cdot \nabla)\mathbf{E}$, where $\Delta' = n_b(\gamma^e - \gamma^m - \gamma^q/6)$ and n_b is the number density of nanospheres. Under illumination with a simple Gaussian beam, the scattered SH intensity distribution consisted of two narrow lobes within the divergence angle of the beam, around the forward direction, with an absence of emission exactly along it, in a very similar profile to the observed angular pattern. Further experiments using two-beam SHG [13] support the mechanism $(\mathbf{E} \cdot \nabla)\mathbf{E}$ behind the nonlinear response of the composite.

These investigations show that the study of quadrupolar SHG becomes important in its own right. The nonlinear response of nanoparticles is of nonlocal character and illustrates well the dependence of SHG on the nature of the exciting field. The SH radiation is determined by the transverse gradient of the incident field, which is null for a plane wave but finite $\sim E/w_0$ for a Gaussian beam (w_0 is the radius of the beam waist). This suggests the use of finite beams to further explore the SHG from centrosymmetric particles and composites. In a previous paper [14] we calculated the SH radiation angular patterns generated by scattering from a homogeneous

*jesusm@cny.unam.mx

centrosymmetric thin composite film, as the one mentioned above, illuminated by a weakly focused laser beam with a transverse field distribution described by linearly polarized Hermite-Gauss (HG) modes. We concentrated mainly on the possibility of SH scattering along the forward direction for a proper combination of two such HG modes in the fundamental field. Beyond the paraxial approximation, SHG of a single centrosymmetric nanosphere excited with tightly focused linearly polarized beams [15] or cylindrical vector beams [16] have been recently reported. Far-field intensity patterns of SHG from a nonlinear crystal with electric-dipole second-order susceptibility tensor were calculated considering excitation with vortex beams with radial and azimuthal polarizations under strong focusing conditions [17–19]. Dipolar SHG with vector Gaussian beams propagating through a nonlinear crystal [20] and surface SHG induced by polarization vortices [21] are additional examples where finite-size beams with inhomogeneous transverse spatial structure and polarization were employed. Recently, multipolar SHG with a focused Gaussian TEM₀₀ beam from a thin nonlinear film have been reported [22]. It was shown that electric-dipole-allowed surface SHG can be interpreted in terms of Mie-type multipoles arising from the atomic-level light-matter interactions and that the interference between these multipoles when excited with a simple Gaussian beam leads to a directional SH emission.

In this paper we study the SHG from a thin composite film with an induced nonlinear quadratic polarization taken as of quadrupolar type $(\mathbf{E} \cdot \nabla)\mathbf{E}$, excited with higher-order Gaussian beams. We extend the study of Ref. [14] to include the excitation with beams having transversely inhomogeneous states of polarization like radially and azimuthally polarized doughnut modes (which are proper combination of HG modes) [23] and helical beams carrying spin and orbital angular momentum (Laguerre-Gauss modes) [24]. These modes are of particular importance for many applications in nano-optics [25], and here we employ them in the context of SH light scattering. Following the theory developed in Ref. [10] we calculate the angular distribution of SH light scattered and show the sensitivity of the quadrupolar SHG to the spatial nature of the polarizing field and to its state of polarization. Bulk quadrupolar SHG under phase matching conditions in an isotropic media excited by HG beams was first considered by Bethune [26]. As for the laser beams with orbital angular momentum (OAM) in the context of second-order nonlinear optical processes, the studies have been restricted to wave mixing in the dipolar approximation. Dipolar SHG by Laguerre-Gaussian beams was observed, evidencing mode transformation to twice the OAM ($l_{2\omega} = 2l_{\omega}$) and conservation of OAM in the light beam, in addition to frequency doubling [27,28]. Also, generation of optical vortex beams from a nonvortex fundamental beam via three-wave mixing in a noncentrosymmetric nonlinear photonic crystal [29] and interaction of optical vortices in a Kerr-like medium [30] were recently reported.

Here we find that the presence of $\nabla\mathbf{E}$ in the nonlinear polarization leads to OAM transformation of the type $l_{2\omega} = 2l_{\omega} + \sigma$, where $\sigma = \pm 1$ is the spin angular momentum of a circularly polarized Laguerre-Gauss exciting field with OAM per photon $l_{\omega}\hbar$. On the other hand, excitation with polarization vortices, such as azimuthally or radially polarized doughnut

modes, leads to transformation of the state of polarization (azimuthal \rightarrow radial) or to the appearance of additional concentric rings in the SH radiation patterns.

II. THEORY

Consider a thin film of width ℓ and lying on the $z = 0$ plane with a nonlinear source polarization [10],

$$\mathbf{P}^{(2)}(\mathbf{r}) = \Delta'(\omega)\mathbf{E} \cdot \nabla\mathbf{E} + \text{nonradiating}, \quad (1)$$

where \mathbf{E} is the driving field and Δ' is the material response function. The scattered SH field in the far zone is given by

$$\mathbf{E}_{2\omega}(\mathbf{r}) = 2q(2q\ell)[\mathbf{P}^{(2)}(\mathbf{K})]^T \frac{e^{i2qr}}{r}, \quad (2)$$

where $q = \omega/c$ is the wave number of the incident field oscillating at the fundamental frequency ω . Assuming that the film is much narrower than the wavelength, $q\ell \ll 1$, and ignoring phase matching effects, the scattering amplitude at 2ω is determined by the transverse (T) part of the two-dimensional Fourier transform,

$$\mathbf{P}^{(2)}(\mathbf{K}) = \int d\mathbf{r}_{\parallel} \mathbf{P}^{(2)}(\mathbf{r}_{\parallel}, z=0) e^{-i\mathbf{K}\cdot\mathbf{r}_{\parallel}}, \quad (3)$$

with wave vector $\mathbf{K} = 2q\hat{\mathbf{n}}_{\parallel} = 2q \sin\theta(\cos\varphi\hat{\mathbf{x}} + \sin\varphi\hat{\mathbf{y}})$, where $\mathbf{r}_{\parallel} = x\hat{\mathbf{x}} + y\hat{\mathbf{y}}$. We assume that at $z = 0$ the driving field is given by the waist of a Gaussian beam and that its width w_0 is much larger than the wavelength, $qw_0 \gg 1$. The beam divergence half-angle $\theta_0 = 2/qw_0 \ll 1$, so that the incident light travels paraxially around the nominal propagation direction z , and thus small variations of order θ_0 in its polarization direction are ignored. We consider x, y as transverse coordinates and then approximate $[\mathbf{P}^{(2)}(\mathbf{K})]^T \approx \mathbf{P}^{(2)}(\mathbf{K})$ [10]. The SH radiated intensity per unit solid angle into direction $\hat{\mathbf{n}}$ is

$$\frac{dI_{2\omega}(\hat{\mathbf{n}})}{d\Omega} = \frac{c}{8\pi}(2q)^2(2q\ell)^2|\Delta'|^2|\mathbf{Q}^{(2)}(\mathbf{K})|^2, \quad (4)$$

where

$$\mathbf{Q}^{(2)}(\mathbf{K}) = \int d\mathbf{r}_{\parallel} e^{-i\mathbf{K}\cdot\mathbf{r}_{\parallel}} \mathbf{E} \cdot \nabla\mathbf{E}, \quad (5)$$

is the vector characterizing the SH scattering amplitude.

A. SH scattering amplitude for a single-mode incident beam

For a single-mode incident beam, we write the exciting field at $z = 0$ as $\mathbf{E}(\mathbf{r}_{\parallel}) = E(x, y)\hat{\mathbf{e}}$ in Cartesian coordinates, or $\mathbf{E}(\mathbf{r}_{\parallel}) = E(\rho, \phi)\hat{\mathbf{e}}$ in polar coordinates, where the constant unitary vector $\hat{\mathbf{e}} \perp \hat{\mathbf{z}}$ gives the polarization of the mode along the xy plane.

Using $\mathbf{E} \cdot \nabla\mathbf{E} = \frac{1}{2}\hat{\mathbf{e}}(\hat{\mathbf{e}} \cdot \nabla E^2)$ and integrating by parts, the vector (5) can be written

$$\mathbf{Q}^{(2)}(\mathbf{K}) = \hat{\mathbf{e}}(\hat{\mathbf{e}} \cdot \mathbf{K}) \frac{i}{2} \int d\mathbf{r}_{\parallel} E^2(\mathbf{r}_{\parallel}) e^{-i\mathbf{K}\cdot\mathbf{r}_{\parallel}}. \quad (6)$$

The problem has been reduced to the calculation of the in-plane Fourier transform of the square of the field. Note that, in contrast to the case of a dipolar nonlinear polarization $\sim E^2$, there is an additional factor $(\hat{\mathbf{e}} \cdot \mathbf{K})$ arising from the gradient of the field.

If the field is a Gaussian beam of the form

$$E(x, y) = E_0 e^{-(x^2+y^2)/w_0^2} f(x)g(y), \quad (7)$$

then the integral in (6) becomes

$$\int d\mathbf{r}_{\parallel} E^2(\mathbf{r}_{\parallel}) e^{-i\mathbf{K}\cdot\mathbf{r}_{\parallel}} = E_0^2 \mathcal{I}_{f(x)}(K_x) \mathcal{I}_{g(y)}(K_y), \quad (8)$$

with

$$\mathcal{I}_{h(x)}(K_x) = \int dx e^{-iK_x x} e^{-2x^2/w_0^2} h^2(x). \quad (9)$$

If the field is expressed in polar coordinates as

$$E(\rho, \phi) = U(\rho) e^{i\ell\phi}, \quad (10)$$

then

$$\int d\mathbf{r}_{\parallel} E^2(\mathbf{r}_{\parallel}) e^{-i\mathbf{K}\cdot\mathbf{r}_{\parallel}} = 2\pi i^{2\ell} e^{i(2\ell)\varphi} \int_0^{\infty} d\rho \rho U^2(\rho) J_{2\ell}(K\rho), \quad (11)$$

where $J_n(x)$ is the Bessel function of the first kind of order n and we have used the identity [25]

$$\int_0^{2\pi} d\phi e^{i2m\phi} e^{-ix \cos(\phi-\varphi)} = 2\pi i^{2m} e^{i2m\varphi} J_{2m}(x). \quad (12)$$

B. SH scattering amplitude for a two-mode incident beam

For a superposition of two Gaussian modes, at the beam waist $z = 0$, $\mathbf{E}(\mathbf{r}_{\parallel}) = E_1(\mathbf{r}_{\parallel})\hat{\mathbf{e}}_1 + E_2(\mathbf{r}_{\parallel})\hat{\mathbf{e}}_2$, the integral (5) gives

$$\begin{aligned} \mathbf{Q}^{(2)}(\mathbf{K}) &= \frac{i}{2} \int d\mathbf{r}_{\parallel} \mathbf{E}(\mathbf{E} \cdot \mathbf{K}) e^{-i\mathbf{K}\cdot\mathbf{r}_{\parallel}} + \frac{1}{2} (\hat{\mathbf{e}}_1 \times \hat{\mathbf{e}}_2) \\ &\times \int d\mathbf{r}_{\parallel} e^{-i\mathbf{K}\cdot\mathbf{r}_{\parallel}} (E_1 \nabla E_2 - E_2 \nabla E_1). \end{aligned} \quad (13)$$

The first term arises from terms involving only ∇E_i^2 or $\nabla(E_i E_j)$ in $(\mathbf{E} \cdot \nabla)\mathbf{E}$ and has the same form as (6), while the second one comes from terms of the form $E_i \nabla E_j$. Note that when $\hat{\mathbf{e}}_1 = \hat{\mathbf{e}}_2$, the last term vanishes and the expression (13) simplifies to (6) with E taken as $E_1 + E_2$.

III. RESULTS

We consider excitation with laser beams in different higher-order transverse modes. The beams of interest in this study are the Hermite-Gaussian modes HG_{lm} and Laguerre-Gaussian modes LG_p^l [31]. At $z = 0$ the former are given by [see Eq. (7)],

$$E(x, y) = \frac{E_{lm}^0}{w_0} e^{-(x^2+y^2)/w_0^2} H_l\left(\frac{\sqrt{2}x}{w_0}\right) H_m\left(\frac{\sqrt{2}y}{w_0}\right), \quad (14)$$

where $H_l(x)$ is the Hermite polynomial of order l , w_0 is the radius of the beam waist, and E_{lm}^0 is the corresponding mode amplitude. The latter are modes LG_p^l in cylindrical coordinates (ρ, ϕ) , which at the beam waist are of the form (10)

$$E(\rho, \phi) = \frac{E_0}{w_0} \left(\frac{\sqrt{2}\rho}{w_0}\right)^l L_p^l(2\rho^2/w_0^2) e^{-\rho^2/w_0^2} e^{i\ell\phi}, \quad (15)$$

where $L_p^l(x)$ is an associated Laguerre polynomial, the integers l and p are azimuthal and radial mode numbers. This beam

carries a well-defined OAM of $l\hbar$ per photon [24]; $p + 1$ gives the number of radial nodes.

In each case, we find that the SH scattering amplitude takes the form $\mathbf{Q}^{(2)}(\boldsymbol{\delta}) = A_0 e^{-\delta^2/4} \mathbf{F}(\boldsymbol{\delta})$, where $A_0 = (E_0/w_0)^2 i\pi w_0/2\sqrt{2}$. Accordingly, in the figures below we plot the function $|\mathbf{Q}^{(2)}(\boldsymbol{\delta})/A_0|^2$, which determines the angular distribution of the SH radiated intensity.

A. Hermite-Gauss and doughnut modes

For a single mode (14) $\mathbf{E}_\omega = \text{HG}_{lm} \hat{\mathbf{e}}$, the integrals (9) can be evaluated to obtain

$$\mathbf{Q}^{(2)}(\boldsymbol{\delta}) = \left(\frac{E_{lm}^0}{w_0}\right)^2 \frac{i\pi w_0}{2\sqrt{2}} e^{-\delta^2/4} [C_{11}(\boldsymbol{\delta}) \hat{\mathbf{e}} \hat{\mathbf{e}}] \cdot \boldsymbol{\delta}, \quad (16)$$

where we have introduced the dimensionless wave vector $\boldsymbol{\delta} = \mathbf{K}w_0/\sqrt{2} \approx \sqrt{8}(\theta/\theta_0)(\cos\varphi\hat{\mathbf{x}} + \sin\varphi\hat{\mathbf{y}})$, giving the angular position of a detector in the far zone. The function $C_{11}(\boldsymbol{\delta})$ is calculated from

$$\begin{aligned} C_{ij}(\boldsymbol{\delta}) &= C_{l_i m_i, l_j m_j}(\boldsymbol{\delta}) = (-i)^\zeta 2^{l_<+m_<-l_>! m_<-!} \delta_x^{l_>-l_<} \\ &\times \delta_y^{m_>-m_<-l_>-l_<} (\delta_x^2/2) L_{m_>-m_<-}^{l_>-l_<} (\delta_y^2/2), \end{aligned} \quad (17)$$

$i, j = 1, 2$, with $p_>(p_<) = \max(\min)\{p_i, p_j\}$, $\zeta = (l_> - l_<) + (m_> - m_<)$. The SH scattering amplitude (16) may be written in terms of HG_{lm} modes after using the formula [24]

$$\sum_{k=0}^{2n} (2i)^k P_k^{(n-k, n-k)}(0) H_{2n-k}(x) H_k(0) = 2^{2n} (-1)^n n! L_n^0(x^2), \quad (18)$$

where

$$P_k^{(n-k, m-k)}(0) = \frac{(-1)^k}{2^k k!} \frac{d^k}{dt^k} [(1-t)^n (1+t)^m] \Big|_{t=0};$$

note that the sum involves only real terms and polynomials of even order, given that $H_k(0) = 0$ for odd k . We obtain

$$\begin{aligned} (-2)^{l+m} C_{11} &= \sum_{p=0}^l \sum_{q=0}^m a_{lm}(p, q) H_{2l-2p}(\delta_x/\sqrt{2}) \\ &\times H_{2m-2q}(\delta_y/\sqrt{2}), \end{aligned} \quad (19)$$

where $a_{lm}(p, q) = (-4)^{p+q} P_{2p}^{(l-2p, l-2p)}(0) P_{2q}^{(m-2q, m-2q)}(0) H_{2p}(0) H_{2q}(0)$, with $p, q = 0, 1, 2, 3, \dots$. This means that the quadrupolar SHG process ‘‘transforms’’ a single-mode incident HG_{lm} beam into a scattered SH field with the same polarization state and an amplitude given by a combination of HG modes of even order, in addition to the gradient factor $(\hat{\mathbf{e}} \cdot \mathbf{K})$; schematically,

$$\begin{aligned} e^{-(x^2+y^2)/w_0^2} H_{lm}(x, y) \hat{\mathbf{e}} &\xrightarrow{\text{shg}} e^{-(K_x^2+K_y^2)w_0^2/8} \\ &\times \left[\sum_{p=0}^l \sum_{q=0}^m a_{lm}(p, q) H_{2l-2p, 2m-2q}(K_x, K_y) \right] (\hat{\mathbf{e}} \cdot \mathbf{K}) \hat{\mathbf{e}}, \end{aligned} \quad (20)$$

with $H_{lm}(x, y) = H_l(x)H_m(y)$. For example, the SH pattern corresponding to the $\text{HG}_{01}\hat{\mathbf{x}}$ incident mode is a superposition of HG_{00} and HG_{02} , similar to the dipolar case [18,19], but

with an extra nodal line given by $\hat{\mathbf{x}} \cdot \mathbf{K} = 0$, as can be seen in Fig. 1(b) of Ref. [14].

For the incident superposition $\mathbf{E} = \text{HG}_{l_1 m_1} \hat{\mathbf{e}}_1 + \text{HG}_{l_2 m_2} \hat{\mathbf{e}}_2$,

$$\mathbf{E}(x, y) = e^{-(x^2+y^2)/w_0^2} \sum_{i=1}^2 \hat{\mathbf{e}}_i \frac{E_{l_i m_i}^0}{w_0} H_{l_i} \left(\frac{\sqrt{2}x}{w_0} \right) H_{m_i} \left(\frac{\sqrt{2}y}{w_0} \right), \quad (21)$$

we obtain from (13) [14], assuming equal amplitudes, $E_{l_1 m_1}^0 = E_{l_2 m_2}^0 = E_0$,

$$\mathbf{Q}^{(2)}(\boldsymbol{\delta}) = \frac{E_0^2}{w_0^2} \frac{i \pi w_0}{2 \sqrt{2}} e^{-\delta^2/4} \times \left[\left(\sum_{i,j=1}^2 C_{ij}(\boldsymbol{\delta}) \hat{\mathbf{e}}_i \hat{\mathbf{e}}_j \right) \cdot \boldsymbol{\delta} + C_{12} \mathbf{T}_{12}(\boldsymbol{\delta}) \right], \quad (22)$$

where

$$\mathbf{T}_{12}(\boldsymbol{\delta}) = 2(\hat{\mathbf{e}}_1 \times \hat{\mathbf{e}}_2) \times [(l_2 - l_1) \delta_x^{-1} \hat{\mathbf{x}} + (m_2 - m_1) \delta_y^{-1} \hat{\mathbf{y}}]. \quad (23)$$

In Ref. [14] we focused on some asymmetric combinations of HG modes in the incident field with $\zeta = 1$ to explore the possibility of SH radiation along the forward direction. This is illustrated in Fig. 1, which shows the SH angular patterns [Figs. 1(b) and 1(d)] produced by the single-mode beam

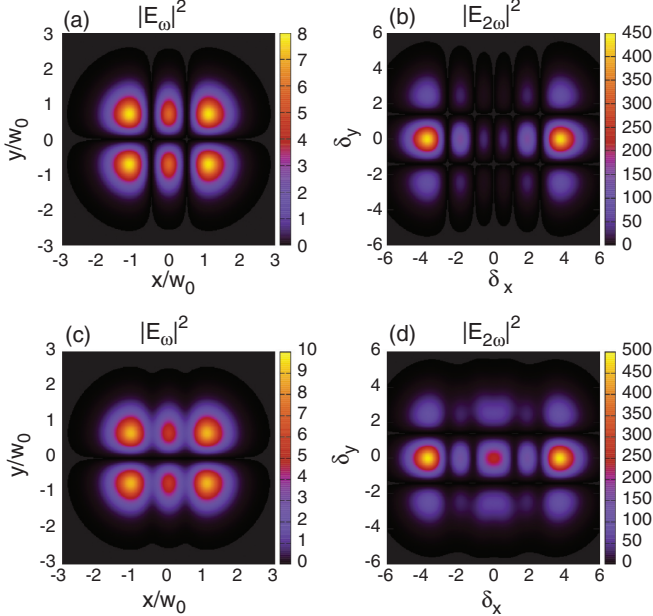


FIG. 1. (Color online) Amplitude patterns $|\mathbf{E}_\omega(x, y)|^2$ of fundamental beam and angular intensity distribution $|\mathbf{E}_{2\omega}(\theta, \varphi)|^2 \propto |\mathbf{Q}^{(2)}(\boldsymbol{\delta})|^2$ of SH light scattered from a thin composite film with the nonlinear polarization source $(\mathbf{E} \cdot \nabla)\mathbf{E}$. (a) Linearly polarized single-mode incident beam $\mathbf{E}_\omega = \text{HG}_{21} \hat{\mathbf{x}}$ and (b) its corresponding SH radiation pattern. (c) Cross-polarized two-mode incident beam $\mathbf{E}_\omega = \text{HG}_{21} \hat{\mathbf{x}} + \text{HG}_{11} \hat{\mathbf{y}}$ and (d) its corresponding SH radiation pattern. The dimensionless angular coordinates in the far zone are $\boldsymbol{\delta} = \sqrt{8}(\theta/\theta_0)(\cos \varphi \hat{\mathbf{x}} + \sin \varphi \hat{\mathbf{y}})$. Here and in the following figures we plot the square modulus of $\mathbf{Q}^{(2)}(\boldsymbol{\delta})/A_0 = e^{-\delta^2/4} \mathbf{F}(\boldsymbol{\delta})$ (see text).

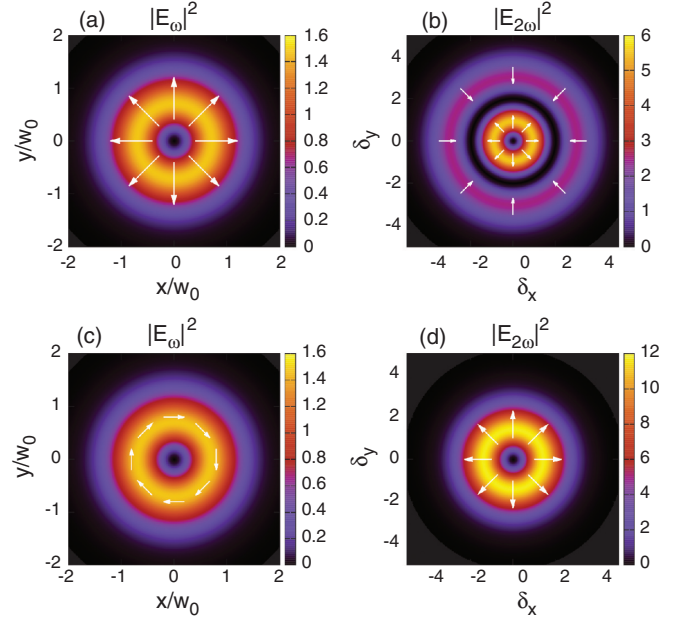


FIG. 2. (Color online) (a) Intensity distribution of a fundamental field given by a radially polarized doughnut mode $\mathbf{E} = \text{HG}_{10} \hat{\mathbf{x}} + \text{HG}_{01} \hat{\mathbf{y}}$ and (b) the corresponding intensity pattern of the scattered SH field. (c) Intensity distribution of a fundamental beam given by an azimuthally polarized doughnut mode $\mathbf{E}_\omega = \text{HG}_{01} \hat{\mathbf{x}} - \text{HG}_{10} \hat{\mathbf{y}}$ and (d) the SH radiated pattern.

$\mathbf{E} = \text{HG}_{21} \hat{\mathbf{x}}$ [Fig. 1(a)] and the cross-polarized superposition $\mathbf{E} = \text{HG}_{21} \hat{\mathbf{x}} + \text{HG}_{11} \hat{\mathbf{y}}$ [Fig. 1(c)].

For a radially polarized doughnut mode $\mathbf{E} = \text{HG}_{10} \hat{\mathbf{x}} + \text{HG}_{01} \hat{\mathbf{y}} \propto e^{-(x^2+y^2)/w_0^2} (x \hat{\mathbf{x}} + y \hat{\mathbf{y}})/w_0$ [Fig. 2(a)] we obtain from (22)

$$\mathbf{Q}^{(2)}(\boldsymbol{\delta}) = \frac{E_0^2}{w_0^2} \frac{i \pi w_0}{2 \sqrt{2}} (4 - \delta^2) e^{-\delta^2/4} \boldsymbol{\delta}. \quad (24)$$

The corresponding SH angular pattern shows two annular rings with alternate radial polarization and radial nodes at angular displacements $\theta = 0$ and $\theta = 0.3\theta_0$, as can be seen in Fig. 2(b).

An azimuthally polarized doughnut mode $\mathbf{E} = \text{HG}_{01} \hat{\mathbf{x}} - \text{HG}_{10} \hat{\mathbf{y}} \propto e^{-(x^2+y^2)/w_0^2} (y \hat{\mathbf{x}} - x \hat{\mathbf{y}})/w_0$ [Fig. 2(c)] generates a vector scattering amplitude with a pure radial dependence,

$$\mathbf{Q}^{(2)}(\boldsymbol{\delta}) = \frac{E_0^2}{w_0^2} \frac{i \pi w_0}{2 \sqrt{2}} 4e^{-\delta^2/4} \boldsymbol{\delta}. \quad (25)$$

In this case the SHG process gives an annular SH distribution with a single ring, but changes the state of polarization from azimuthal to radial [Fig. 2(d)].

B. Laguerre-Gauss modes

Under excitation with a Laguerre-Gauss mode (15) $\mathbf{E} = \text{LG}_p^l \hat{\mathbf{e}}$, the harmonic vector amplitude (6) can be obtained by evaluating the integral (11),

$$\mathbf{Q}^{(2)}(\boldsymbol{\delta}) = \hat{\mathbf{e}} \frac{E_0^2}{w_0^2} \frac{i \pi w_0}{2 \sqrt{2}} (\hat{\mathbf{e}} \cdot \boldsymbol{\delta}) e^{i2l\varphi} (-1)^l 2 \times \int_0^\infty dx x^{2l+1} e^{-x^2} [L_p^l(x^2)]^2 J_{2l}(x\boldsymbol{\delta}); \quad (26)$$

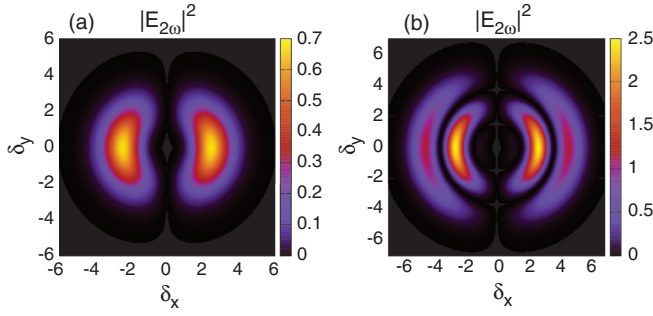


FIG. 3. (Color online) SH intensity distributions generated by scattering from a thin composite film for linearly polarized single-mode LG beams: (a) $\mathbf{E}_\omega = \text{LG}_0^1 \hat{x}$ and (b) $\mathbf{E}_\omega = \text{LG}_1^1 \hat{x}$.

this can be done analytically for arbitrary mode numbers l and p [32]. Here we present expressions corresponding to $p = 0$ and $p = 1$. Given that $\text{LG}_0^l(x) = 1$, the integral (11) when $p = 0$ simplifies to yield

$$\mathbf{Q}^{(2)}(\delta) = \frac{E_0^2}{w_0^2} \frac{i}{2} \frac{\pi w_0}{\sqrt{2}} \frac{(-1)^l}{2^{2l}} \delta^{2l} e^{i2l\varphi} e^{-\delta^2/4} (\hat{\mathbf{e}} \cdot \delta) \hat{\mathbf{e}}. \quad (27)$$

When $\mathbf{E}_\omega = \text{LG}_1^l \hat{\mathbf{e}}$, an additional factor appears in the transverse structure of the SH far field,

$$\begin{aligned} \mathbf{Q}^{(2)}(\delta) &= \frac{E_0^2}{w_0^2} \frac{i}{2} \frac{\pi w_0}{\sqrt{2}} \frac{(-1)^l}{2^{2l}} \delta^{2l} e^{i2l\varphi} \\ &\times \frac{1}{2} [l + 1 - L_2^{2l}(\delta^2/2)] e^{-\delta^2/4} (\hat{\mathbf{e}} \cdot \delta) \hat{\mathbf{e}}. \end{aligned} \quad (28)$$

Figure 3 shows the SH radiation patterns generated by the linearly polarized doughnut modes (a) $\mathbf{E} = \text{LG}_0^1 \hat{x} = \text{HG}_{10} \hat{x} + i\text{HG}_{01} \hat{y}$ and (b) $\mathbf{E} = \text{LG}_1^1 \hat{x}$. In contrast, for circular polarization $\hat{\mathbf{e}} = \hat{\sigma}_\pm = \frac{1}{\sqrt{2}}(\hat{x} \pm i\hat{y})$, the gradient factor becomes $(\hat{\mathbf{e}} \cdot \mathbf{K}) = \frac{1}{\sqrt{2}}(K_x \pm iK_y) = \frac{1}{\sqrt{2}}K e^{\pm i\varphi}$ and introduces an additional phase in the SH field. This means that for a circularly polarized input beam with a spiral phase wave front, with orbital helicity (or topological charge) l and spin helicity $\sigma = \pm 1$, the SHG via $\nabla \mathbf{E}$ process generates a circularly polarized vortex field $\mathbf{E}_{2\omega}$ with charge $l_{2\omega} = 2l \pm 1$ and the same spin. Invoking conservation of total angular momentum per photon energy, $J_{2\omega} = 2J_\omega = 2(l_\omega + \sigma)$, this mode transformation via SHG corresponds to $J_{2\omega} = l_{2\omega} + \sigma$ with a spin-dependent selection rule $l_{2\omega} = 2l_\omega + \sigma$ for the OAM doubling. This is in contrast to the case of linear polarization $\hat{\mathbf{e}} = \cos \alpha \hat{x} + \sin \alpha \hat{y}$, where $(\hat{\mathbf{e}} \cdot \mathbf{K}) = K \cos(\varphi - \alpha)$, which merely introduces a nodal line at $\varphi = \alpha + \pi/2$, as can be seen in Fig. 3. In particular, the above rule then implies that an incident simple Gaussian beam without OAM, $\text{LG}_0^0 \hat{\sigma}_\pm$, would produce a SH vortex with $l = \pm 1$, depending on the polarization handedness (spin) of the fundamental field; the case $p = l = 0$ and $\sigma = +1$ is shown in Fig. 4. This particular case of mode transformation ($l = 0 \rightarrow l = 1$) was observed in SHG in air and explained in terms of the inhomogeneous distribution of the electron density

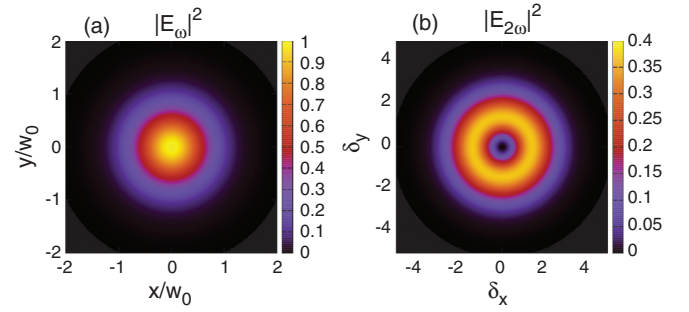


FIG. 4. (Color online) (a) Intensity pattern of an incident simple Gaussian field $\mathbf{E}_\omega = \text{LG}_0^0 \hat{\sigma}_+$, without OAM. (b) The corresponding scattered SH field is a circularly polarized optical vortex with charge $l = 1$.

created by a ponderomotive force associated to a transverse gradient $\nabla_\perp E^2$ [33,34].

IV. CONCLUSIONS

We have calculated the vector scattering amplitude of the far field at the second harmonic generated by a thin composite film with a nonlinear polarization source of quadrupolar type $(\mathbf{E} \cdot \nabla)\mathbf{E}$. The exciting field is a higher-order Gaussian beam with a transverse spatial structure given by Hermite or Laguerre modes. For a single-mode incident beam the presence of $\nabla \mathbf{E}$ introduces the factor $\mathbf{E}(\mathbf{E} \cdot \mathbf{K})$ in the Fourier component that gives the scattering amplitude. This factor is absent in electric-dipole-allowed SHG and we showed that it can give additional nodal lines or rings in the SH angular patterns, changes of the state of polarization, or additional azimuthal phases in the SH radiated field, depending on the transverse structure and polarization of the fundamental beam. We show that, for a linearly polarized $\text{HG}_{lm} \hat{\mathbf{e}}$ beam, the quadrupolar SH scattering gives a SH field which can be written as a superposition of HG modes of even order, with the overall gradient factor $\hat{\mathbf{e}} \cdot \mathbf{K}$. For a two-mode incident beam, the SH radiated field contains an additional contribution given by the 2D Fourier transform of mixed terms like $E_i \nabla E_j$ in the nonlinear polarization and which is null for modes with collinear polarization. For radially polarized doughnut mode, the angular intensity distribution of the scattered SH field shows two concentric rings with alternate radial polarization, while for an azimuthally polarized beam it shows a single annular ring pattern but with radial polarization. These examples illustrate well the sensitivity of quadrupolar SHG to the state of polarization of the exciting field, besides the transverse spatial structure. When a circularly polarized vortex beam $\text{LG}_p^l \hat{\sigma}_\pm$ is used, we find a SH scattered field with an azimuthal phase structure of the form $e^{i(2l \pm 1)\varphi}$, evidencing the generation of a frequency-doubled helical beam with OAM per photon $(2l \pm 1)\hbar$. This suggests a selection rule where a fundamental field given by an optical vortex with charge l_ω and spin helicity $\sigma = \pm 1$ induces a SH vortex field with charge $l_{2\omega} = 2l_\omega + \sigma$ and the same state of polarization σ . In the quadrupolar SHG studied here, the nonlinear scattering of a circularly polarized beam with spiral phase wave front results in a spin-dependent doubling of the OAM. This is in contrast to the process $l_{2\omega} \rightarrow 2l_\omega$, observed in dipolar

SHG [27,28], and it represents an alternative way to double the OAM. The distinctive features of the patterns shown here become characteristic signatures which may be useful to identify a SHG process of quadrupolar nature or to produce directional SH emission with a particular state of polarization in a desired radiation pattern. Creation of vortices by a quadrupolar nonlinear light scattering could find application

in vortex-control mechanisms. We hope that this work will stimulate further experiments and theory.

ACKNOWLEDGMENT

We acknowledge the support from DGAPA-UNAM under Grant No. IN114210.

-
- [1] T. F. Heinz, in *Nonlinear Surface Electromagnetic Phenomena*, edited by H.-E. Ponath and G. I. Stegeman (Elsevier, Amsterdam, 1991), p. 354.
 - [2] G. A. Reider and T. F. Heinz, in *Photonic Probes of Surfaces*, edited by P. Halevi (Elsevier, Amsterdam, 1995), Chap. 9.
 - [3] J. E. McGilp, *Surf. Rev. Lett.* **6**, 529 (1999).
 - [4] G. Lüpke, *Surf. Sci. Rep.* **35**, 75 (1999).
 - [5] M. C. Downer, B. S. Mendoza, and V. I. Gavrilenko, *Surf. Interface Anal.* **31**, 966 (2001).
 - [6] M. B. Raschke and Y. R. Shen, *Curr. Opin. Solid State Mater. Sci.* **8**, 343 (2004).
 - [7] K. Pedersen, *Phys. Status Solidi B* **247**, 2002 (2010).
 - [8] S. Roke and G. Gonella, *Annu. Rev. Phys. Chem.* **63**, 353 (2012), and references therein.
 - [9] J. I. Dadap, J. Shan, K. B. Eisenthal, and T. F. Heinz, *Phys. Rev. Lett.* **83**, 4045 (1999); J. I. Dadap, J. Shan, and T. F. Heinz, *J. Opt. Soc. Am. B* **21**, 1328 (2004).
 - [10] W. L. Mochán, A. Maytorena, B. S. Mendoza, and V. L. Brudny, *Phys. Rev. B* **68**, 085318 (2003).
 - [11] Y. Jiang, P. T. Wilson, M. C. Downer, C. W. White, and S. P. Withrow, *Appl. Phys. Lett.* **78**, 766 (2001).
 - [12] J. Wei, A. Wirth, M. C. Downer, and B. S. Mendoza, *Phys. Rev. B* **84**, 165316 (2011).
 - [13] P. Figliozzi, L. Sun, Y. Jiang, N. Matlis, B. Mattern, M. C. Downer, S. P. Withrow, C. W. White, W. L. Mochán, and B. S. Mendoza, *Phys. Rev. Lett.* **94**, 047401 (2005).
 - [14] R. Bernal and J. A. Maytorena, *Phys. Rev. B* **70**, 125420 (2004).
 - [15] B. Huo, X. Wang, S. Chang, M. Zeng, and G. Zhao, *J. Opt. Soc. Am. B* **28**, 2702 (2011).
 - [16] B. Huo, X. Wang, S. Chang, and M. Zeng, *J. Opt. Soc. Am. B* **29**, 1631 (2012).
 - [17] A. Ohtsu, Y. Kozawa, and S. Sato, *Appl. Phys. B* **98**, 851 (2010).
 - [18] A. Ohtsu, *Opt. Commun.* **283**, 3831 (2010).
 - [19] Y. Kozawa and S. Sato, *J. Opt. Soc. Am. B* **25**, 175 (2008).
 - [20] S. Carrasco, B. E. A. Saleh, M. C. Teich, and J. T. Fourkas, *J. Opt. Soc. Am. B* **23**, 2134 (2006).
 - [21] D. P. Biss and T. G. Brown, *Opt. Lett.* **28**, 923 (2003).
 - [22] M. J. Huttunen, J. Mäkitalo, G. Bautista, and M. Kauranen, *New J. Phys.* **14**, 113005 (2012).
 - [23] Q. Zhan, *Adv. Opt. Photon.* **1**, 1 (2009).
 - [24] L. Allen, M. W. Beijersbergen, R. J. C. Spreeuw, and J. P. Woerdman, *Phys. Rev. A* **45**, 8185 (1992).
 - [25] L. Novotny and B. Hecht, *Principles of Nano-optics* (Cambridge University Press, Cambridge, UK, 2006).
 - [26] D. S. Bethune, *Opt. Lett.* **6**, 287 (1981).
 - [27] K. Dholakia, N. B. Simpson, M. J. Padgett, and L. Allen, *Phys. Rev. A* **54**, R3742 (1996).
 - [28] J. Courtial, K. Dholakia, L. Allen, and M. J. Padgett, *Phys. Rev. A* **56**, 4193 (1997).
 - [29] A. Bahabad and A. Arie, *Opt. Exp.* **15**, 17619 (2007).
 - [30] F. Lenzini, S. Residori, F. T. Arecchi, and U. Bortolozzo, *Phys. Rev. A* **84**, 061801(R) (2011).
 - [31] E. J. Galvez, *Am. J. Phys.* **74**, 355 (2006).
 - [32] I. S. Gradshteyn and I. M. Ryzhik, *Table of Integrals, Series, and Products* (Academic Press, New York, 1965), integral 7.422.1, p. 848.
 - [33] M. Beresna, P. G. Kazansky, Y. Svirko, M. Barkauskas, and R. Danielius, *Appl. Phys. Lett.* **95**, 121502 (2009).
 - [34] D. F. Gordon, B. Hafizi, and A. Ting, *Opt. Lett.* **34**, 3280 (2009).